© 1998 The Chemical Society of Japan Bull. Chem. Soc. Jpn., 71, 1363—1371 (1998) 1363

Synthesis, Crystal Structures, and Properties of S-Bridged Pt(II)-Ni(II) Dinuclear Complexes: Conversion of Square-Planar [Ni(aet)$_2$] to Octahedral Geometry by Forming an S-Bridged Structure with Pt(II) (aet=2-Aminoethanethiolate)

Ken-ichi Okamoto,* Yukie Yoshinari, Yasunori Yamada, Narumi Sakagami, and Takumi Konno[†]

Department of Chemistry, University of Tsukuba, Tsukuba 305-8571

†Department of Chemistry, Faculty of Engineering, Gunma University, Kiryu, Gunma 376-8516

(Received December 10, 1997)

The reactions of [Ni(aet)$_2$] with [PtCl$_2$(L)] gave a new type of S-bridged dinuclear complexes [Pt(L){Ni(aet)$_2$(H$_2$O)$_2$}]$^{2+}$ (aet=aminoethanethiolate; L=bpy=2,2′-bipyridine, phen=1,10-phenanthroline (**5**), dmbpy=4,4′-dimethyl-2,2′-bipyridine). These complexes readily react with L′ to form [M(L){Ni(aet)$_2$(L′)}]$^{2+}$ (L=bpy, L′=bpy (**3**), phen; L=phen, L′=phen, bpy; L=L′=dmbpy). A similar reaction of [Ni(aet)$_2$] with [PtCl$_2$(phen)] and phen gave only [Pt(phen){Ni(aet)$_2$(phen)}]$^{2+}$. The crystal structures of **3** and **5** were determined by X-ray crystallography. The Ni atoms are surrounded by two aet and a bpy or two water molecules to have an approximately octahedral geometry, forming the C$_2$-*cis*(*S*)-[Ni(aet)$_2${bpy or (H$_2$O)$_2$}] unit. The Pt atoms have a square-planar geometry, in which two Cl atoms of the starting [PtCl$_2$(L)] (L=bpy or phen) have been substituted by the two S atoms from the Ni(II) unit. The Pt(II) plane and the Ni(II) equatorial plane are almost coplanar, and the Pt–Ni distance is 3.4987(8) Å (**3**) and 3.476(4) Å (**5**). All of the complexes were characterized on the basis of the electronic absorption and infrared spectra and the cyclic voltammetry. The conversion of a square-planar [Ni(aet)$_2$] to an octahedral [Ni(aet)$_2${(H$_2$O)$_2$ or (L′)}] units was also considered. In the solid state, the water molecule in [Pt(L){Ni(aet)$_2$(H$_2$O)$_2$}]$^{2+}$ could be readily exchanged by nitrate.

The binding ability of the thiolato sulfur atoms coordinated to other metal ions has led to the development of stereochemistry of S-bridged polynuclear complexes, several of which have been derived from square-planar [M(thiolato-S)$_2$(amine-N)$_2$]-type (M=Ni$^{\mathrm{II}}$, Pd$^{\mathrm{II}}$) mononuclear complexes.[1—15] Of these polynuclear complexes, most of the [M(thiolato-S)$_2$(amine-N)$_2$]-type complexes can function as S-donating metalloligands. For example, the reaction of [Ni(aet)$_2$] (aet=2-aminoethanethiolate) with NiCl$_2$ gave a linear-type S-bridged trinuclear complex, [Ni{Ni(aet)$_2$}$_2$]$^{2+}$, in which each square-planar *cis*(*S*)-[Ni(aet)$_2$] unit chelates to one Ni(II) ion.[1—3] Further, the reaction of [Ni(aet)$_2$] with Na$_2$PdCl$_4$ gave stereoselectively the pin-wheel-type hexanuclear S-bridged complexes, [Pd$_2${Ni(aet)$_2$}$_4$]$^{4+}$, in which each square-planar *cis*(*S*)-[Ni(aet)$_2$] unit spans to two Pd(II) ions.[15] When the mononuclear complexes [MCl$_2$(L)] (M=Pt$^{\mathrm{II}}$, Pd$^{\mathrm{II}}$), in which the ligands L (=2,2′-bipyridine (bpy), 1,10-phenanthroline (phen), and 4,4′-dimethyl-2,2′-bipyridine (dmbpy)) are less susceptible to substitution of other ligands, reacts with [Ni(aet)$_2$], therefore, it will be expected that the dinuclear complexes, [M(L){Ni(aet)$_2$}]$^{2+}$, or tetranuclear complexes, [{M(L)}$_2${Ni(aet)$_2$}$_2$]$^{4+}$, are formed, which contain square-planar *cis*(*S*)-[Ni(aet)$_2$] units. Recently, however, we presented a preliminary result that the reaction of [Ni(aet)$_2$] with [PtCl$_2$(bpy)] produced a new type of dinuclear complexes [Pt(bpy){Ni(aet)$_2$(H$_2$O)$_2$}]$^{2+}$, in which the Ni(II) ion does not have a square-planar coordination geometry, but converts to an octahedral geometry.[16] Further, [Pt(bpy){Ni(aet)$_2$(H$_2$O)$_2$}]$^{2+}$ readily reacts with bpy to form [Pt(bpy){Ni(aet)$_2$(bpy)}]$^{2+}$.[16] In this paper we report on a detailed study concerning the syntheses, structures, and chemical characterizations of the S-bridged dinuclear complexes [Pt(L){Ni(aet)$_2$(H$_2$O)$_2$}]$^{2+}$, [Pt(L){Ni(aet)$_2$(L′)$_2$}]$^{2+}$, and [Pd(phen){Ni(aet)$_2$(phen)}]$^{2+}$ (L,L′=bpy, phen, dmbpy). The geometrical conversion about the Ni(II) ion is also discussed in relation to the geometry or the reactivity around the metal ions.

Experimental

Materials. Sodium tetrachloropalladate(II) was purchased from Aldrich Chemical Co., Inc. The other reagents were purchased from Wako Pure Chemical Ind. Co., Ltd., and Tokyo Chemical Co., Ltd. All of the chemicals were of reagent grade and used without further purification.

Preparation of Complexes. ***trans*(*S*)-[Ni(aet)$_2$].** This complex was prepared by a method similar to that described in the literature.[1] The yield was nearly quantitative: 98.6%.

[PtCl$_2$(bpy)]. This complex was prepared by a method similar to that described in the literature,[17,18] using a solution containing 2.0 g (4.8 mmol) of potassium tetrachloroplatinate(II) in 250 cm^3 of water, 0.78 g (5.0 mmol) of 2,2′-bipyridine, and 10 cm^3 of 2 mol dm^{-3} hydrochloric acid. Yield: 95%.

[PtCl$_2$(phen)]. This complex was prepared by a method similar to that for $[PtCl_2(bpy)]$, using a solution containing 1.0 g (2.4 mmol) of potassium tetrachloroplatinate(II) in 100 cm^3 of water, 0.54 g (2.7 mmol) of 1,10-phenanthroline monohydrate, and 4 cm^3 of 2 mol dm^{-3} hydrochloric acid. Yield: 97.7%. Calcd for $C_{12}H_8N_2Cl_2Pt$: C, 32.30; H, 1.81; N, 6.28%. Found: C, 32.45; H, 1.87; N, 6.32%.

$[PtCl_2(dmbpy)]$. This complex was also prepared by a method similar to that for $[PtCl_2(bpy)]$, using 4,4′-dimethyl-2,2′-bipyridine (2.7 mmol) instead of 2,2′-bipyridine (2.5 mmol). Yield: 99.6%. Calcd for $C_{12}H_{12}N_2Cl_2Pt$: C, 32.01; H, 2.69; N 6.22%. Found: C, 31.98; H, 2.63; N, 6.13%.

$[PdCl_2(phen)]$. To a solution containing 0.30 g (1.0 mmol) of sodium tetrachloropalladate(II) in 50 cm^3 of water were added 0.20 g (1.0 mmol) of 1,10-phenanthroline monohydrate and 2 cm^3 of 2 mol dm^{-3} hydrochloric acid. When the mixture was stirred at 80 °C for 30 min, white-orange needles began to appear, and the solution became filled with a mass of filamentous white-orange needles. After standing at room temperature for several hours, the resulting white-orange needles were collected by filtration and washed well with a large amount of water and then methanol. Yield: 0.36 g (99%). Calcd for $C_{12}H_8N_2Cl_2Pd$: C, 40.31; H, 2.26; N, 7.84%. Found: C, 40.31; H, 2.26; N, 7.78%.

$[Pt(bpy)\{Ni(aet)_2(H_2O)(X)\}]^{n+}$ ($\{X, n\}=\{H_2O, 2\}$ for 1; $\{NO_3, 1\}$ for 2). To a yellow suspension containing 0.10 g (0.24 mmol) of $[PtCl_2(bpy)]$ in 10 cm^3 of water was added 0.05 g (0.24 mmol) of $[Ni(aet)_2]$. The mixture was stirred at 50 °C for 20 min, whereupon the mixture became a yellow-brown solution. After removing any unreacted materials by filtration, to the yellow-brown filtrate was added 1.5 cm^3 of a saturated $NaNO_3$ solution. The mixture was allowed to stand at room temperature for 1 d, and the resulting yellow-brown crystals (**1**) were collected by filtration. Yield: 0.10 g (58%). Calcd for $[Pt(bpy)\{Ni(aet)_2(H_2O)_2\}](NO_3)_2=C_{14}H_{24}N_6S_2O_8NiPt$: C, 23.28; H, 3.35; N, 11.64; Ni, 8.13; Pt, 27.01%. Found: C, 23.25; H, 3.26; N, 11.57; Ni, 8.50; Pt, 27.48%.

2 was prepared by the same method as that used for **1**, using 3 cm^3 of a saturated $NaNO_3$ solution. Yield: 0.09 g, Calcd for $[Pt(bpy)\{Ni(aet)_2(NO_3)(H_2O)\}](NO_3)$: C, 23.88; H, 3.15; N, 11.93%. Found: C, 23.64; H, 3.09; N, 11.91%.

$[Pt(bpy)\{Ni(aet)_2(bpy)\}]^{2+}$ (3). To a solution containing 0.10 g (0.14 mmol) of **1** in 10 cm^3 of water was added 0.024 g (0.15 mmol) of 2,2′-bipyridine. The mixture was stirred at 50 °C for 5 min, whereupon the color of the solution readily changed from yellow-brown to red-brown. To the solution was added a few drops of a saturated $NaNO_3$ solution, followed by standing at room temperature for ca. 5 h. The resulting red-brown microcrystals (**3**) were collected by filtration. Recrystallization from water gave red-brown crystals, one of which was used for X-ray structural analysis. Yield: 0.08 g (67%). Calcd for $[Pt(bpy)\{Ni(aet)_2(bpy)\}](NO_3)_2\cdot H_2O=C_{24}H_{30}N_8S_2O_7NiPt$: C, 33.50; H, 3.51; N, 13.02; Ni, 6.82; Pt, 22.67%. Found: C, 33.30; H, 3.41; N, 12.91; Ni, 6.83; Pt, 22.63%.

$[Pt(bpy)\{Ni(aet)_2(phen)\}]^{2+}$ (4). To a solution containing 0.10 g (0.14 mmol) of **1** in 10 cm^3 of water was added 0.028 g (0.14 mmol) of 1,10-phenanthroline. The mixture was stirred at 50 °C for 5 min, whereupon the color of the solution readily changed from yellow-brown to red-brown. The reaction solution was left at room temperature for ca. 5 h. The resulting orange-beige powder (**4**) was collected by filtration. Yield: 0.096 g (77%). Calcd for $[Pt(bpy)\{Ni(aet)_2(phen)\}](NO_3)_2\cdot 1.5H_2O=C_{26}H_{31}N_8S_2O_{7.5}NiPt$: C, 34.95; H, 3.50; N, 12.54%. Found: C, 34.79; H, 3.50; N, 12.38%.

$[Pt(phen)\{Ni(aet)_2(H_2O)(X)\}]^{n+}$ ($\{X, n\}=\{H_2O, 2\}$ for 5; $\{NO_3, 1\}$ for 6). To a yellow suspension containing 0.10 g (0.22 mmol) of $[PtCl_2(phen)]$ in 14 cm^3 of water was added 0.05 g (0.24 mmol) of $[Ni(aet)_2]$. The mixture was stirred at 70 °C for 40 min, whereupon the mixture became a brown solution. After removing a small amount of unreacted materials by filtration, to the brown filtrate was added 0.3 cm^3 of a saturated NaBr solution. The mixture was allowed to stand at room temperature overnight; the resulting brown crystals (**5**) were collected by filtration. One of **5** was used for an X-ray structural analysis. Yield: 0.04 g (23%). Calcd for $[Pt(phen)\{Ni(aet)_2(H_2O)_2\}]BrCl\cdot 1.5H_2O=C_{16}H_{27}N_4S_2O_{3.5}BrClNiPt$: C, 25.13; H, 3.56; N, 7.33%. Found; C, 25.62; H, 3.57%; N, 7.18%. To the filtrate was added 1 cm^3 of a saturated NaBr solution. The mixture was allowed to stand at room temperature for 6 h, and the resulting brown crystals (Br_2 salt of **5**) were collected by filtration. Yield: 0.06 g (33%). Calcd for $[Pt(phen)\{Ni(aet)_2(H_2O)_2\}]Br_2\cdot 1.5H_2O$: C, 23.75; H, 3.36; N, 6.92; Ni, 7.25; Pt, 24.11%. Found: C, 23.61; H, 3.34; N, 6.73; Ni, 7.05; Pt, 23.96%.

6 was prepared by the same method as that used for the BrCl or Br_2 salts of **5**. After removing a small amount of unreacted materials by filtration, to the brown filtrate was added 1 cm^3 of a saturated $NaNO_3$ solution. The mixture was allowed to stand at room temperature overnight, and the resulting brown crystals (**6**) were collected by filtration. Yield: 0.14 g (86%). Calcd for $[Pt(phen)\{Ni(aet)_2(NO_3)(H_2O)\}](NO_3)=C_{16}H_{22}N_6S_2O_7NiPt$: C, 26.39; H, 3.04; N, 11.54%. Found: C, 26.18; H, 3.04; N, 11.41%.

$[Pt(phen)\{Ni(aet)_2(phen)\}]^{2+}$ (7). To a brown solution containing 0.13 g (0.18 mmol) of **6** in 20 cm^3 of water was added 0.04 g (0.20 mmol) of 1,10-phenanthroline monohydrate. The mixture was stirred at 55 °C for 10 min, whereupon the color of the solution changed from brown to red-brown. To the reaction solution was added one drop of a saturated $NaNO_3$ solution, followed by leaving at room temperature for 1 d. From this solution red-brown microcrystals (**7**) were appeared and were collected by filtration. One of the crystals was used for an X-ray analysis. Yield: 0.09 g (54%). Calcd for $[Pt(phen)\{Ni(aet)_2(phen)\}](NO_3)_2\cdot 2.5H_2O=C_{28}H_{33}N_8S_2O_{8.5}NiPt$: C, 35.95; H, 3.56; N, 11.98; Ni, 6.27; Pt, 20.85%. Found: C, 35.67; H, 3.51; N, 11.81; Ni, 6.23; Pt, 20.24%.

$[Pt(phen)\{Ni(aet)_2(bpy)\}]^{2+}$ (8). To a solution containing 0.10 g (0.12 mmol) of the Br_2 salt of **5** in 10 cm^3 of water was added 0.02 g (0.13 mmol) of 2,2′-bipyridine. The mixture was stirred at 50 °C for 5 min, whereupon the color of the solution readily changed from brown to red-brown. The reaction solution was left at room temperature for 1 d. The resulting beige-brown powder (**8**) was collected by filtration. Yield: 0.09 g (76%). Calcd for $[Pt(phen)\{Ni(aet)_2(bpy)\}]Br_2\cdot 8H_2O=C_{26}H_{44}N_6S_2O_8Br_2NiPt$: C, 29.84; H, 4.24; N, 8.03%. Found: C, 29.30; H, 4.22; N, 7.80%.

$[Pt(dmbpy)\{Ni(aet)_2(H_2O)(X)\}]^{n+}$ ($\{X, n\}=\{H_2O, 2\}$ for 9; $\{NO_3, 1\}$ for 10). To a yellow suspension containing 0.05 g (0.11 mmol) of $[PtCl_2(dmbpy)]$ in 10 cm^3 of water was added 0.025 g (0.13 mmol) of $[Ni(aet)_2]$. The mixture was stirred at 50 °C for 40 min, whereupon the mixture became a yellow-brown solution. After removing a small amount of unreacted materials by filtration, to the yellow-brown filtrate was added ca. 1.5 cm^3 of a saturated NaBr solution. The mixture was allowed to stand at room temperature overnight, and the resulting brown crystals (**9**) were collected by filtration. Yield: 0.07 g (77%). Calcd for $[Pt(dmbpy)\{Ni(aet)_2(H_2O)_2\}]Br_2\cdot H_2O=C_{16}H_{30}N_4S_2O_3Br_2NiPt$: C, 23.90; H, 3.76; N, 6.97; Ni, 7.30; Pt, 24.26%. Found: C, 23.83; H, 3.86; N, 6.86; Ni, 6.74; Pt, 23.98%.

The nitrate salt of **10** was obtained by the same method as that used for the bromide salt, using ca. 2.5 cm^3 of a saturated $NaNO_3$ solution instead of a saturated NaBr solution. Yield: 0.056 g (68%). Calcd for $[Pt(dmbpy)\{Ni(aet)_2(NO_3)(H_2O)\}](NO_3)=C_{16}H_{26}N_6S_2O_7NiPt$: C, 26.24; H, 3.58; N, 11.48%. Found: C, 26.24; H, 3.63; N, 11.38%.

$[Pt(dmbpy)\{Ni(aet)_2(dmbpy)\}]^{2+}$ (11). To a brownish-yellow solution containing 0.09 g (0.12 mmol) of **10** in 30 cm^3 of water was added 0.026 g (0.14 mmol) of 4,4′-dimethyl-2,2′-bipyridine. The mixture was stirred at 55 °C for 2 h, whereupon the mixture became a orange-yellow solution. After removing a small amount of unreacted materials by filtration, to the orange-yellow filtrate was added one drop of a saturated $NaNO_3$ solution. The solution was allowed to stand at room temperature for 2 d, and the resulting brown crystals (**11**) were collected by filtration. Yield: 0.045 g (38%). Calcd for $[Pt(dmbpy)\{Ni(aet)_2(dmbpy)\}](NO_3)_2\cdot 5H_2O=C_{28}H_{46}N_8S_2O_{11}NiPt$: C, 34.02; H, 4.69; N, 11.33; Ni, 5.94; Pt, 19.73%. Found: C, 33.93; H, 4.41; N, 11.21; Ni, 6.23; Pt, 19.45%.

$[Pd(phen)\{Ni(aet)_2(phen)\}]^{2+}$ (12). To a pale orange-white suspension containing 0.08 g (0.22 mmol) of $[PdCl_2(phen)]$ in 20 cm^3 of a 1 : 1 methanol/water mixture was added 0.05 g (0.24 mmol) of $[Ni(aet)_2]$. After the mixture was stirred at 40 °C for 15 min, 0.04 g (0.22 mmol) of 1,10-phenanthroline was added with stirring at 40 °C, and continued to be stirred for 5 min. To the reaction solution was added a few drops of a saturated aqueous NaBr solution, followed by leaving at room temperature for 1 d. From this solution the red-brown microcrystals (**12**) appeared and were collected by filtration. Yield: 0.15 g (75%). Calcd for $[Pd(phen)\{Ni(aet)_2(phen)\}]Br_2\cdot 4H_2O = C_{28}H_{36}N_6S_2O_4Br_2NiPd$: C, 36.97; H, 3.99; N, 9.24; Ni, 6.45; Pd, 11.70%. Found: C, 37.08; H, 3.97; N, 9.14; Ni, 5.76; Pd, 11.95%.

Measurements. The electronic absorption spectra were recorded with a JASCO Ubest V-570 spectrophotometer, and the CD spectra with a JASCO J-600 spectropolarimeter. All of the measurements were carried out in aqueous solutions at room temperature. Electrochemical measurements were made with a CV-1B apparatus (Bioanalytical Systems, Inc.; BSI) using a glassy-carbon working electrode and a platinum microelectrode (BSI). An aqueous Ag/AgCl/NaCl (3 mol dm^{-3}) electrode (BSI) and a platinum wire were used as reference and auxiliary electrodes, respectively. Electrochemical experiments were conducted at room temperature in a 0.1 mol dm^{-3} Na_2SO_4 aqueous solution as the supporting electrolyte and complex concentrations of 1.0 mmol dm^{-3}. The concentrations of Ni, Pd, and Pt in the complexes were determined with a Nippon Jarrel-Ash ICPA-575 ICP spectrophotometer. The magnetic susceptibilities were measured with a Sherwood Scientific apparatus at 23 °C. The molar conductances of the complexes were measured with a Horiba conductivity meter DS-14 in aqueous solution at room temperature. The infrared spectra were recorded as KBr disk with a JASCO FT/IR spectrometer.

X-Ray Structure Determination. The unit-cell parameters and intensity data for **3** and **5** were measured on an Enraf Nonius CAD4 diffractometer by using graphite-monochromatized Mo $K\alpha$ radiation ($\lambda = 0.71073$ Å). The unit-cell dimensions were determined by a least-squares refinement of 25 reflections with $16° < 2\theta < 20°$. Crystal data and the experimental parameters are listed in Table 1. The intensity data were collected by the ω–2θ scan technique. The reflections of $F_o > 3\sigma(F_o)$ were used for structure determinations. Data reduction and the application of Lorents, polarization, decomposition (correction factor on I; 1.00—1.00 for **3**; 1.00—1.11 for **5**), and empirical absorption corrections (transmission coefficient on I; 0.65—1.00 for **3**; 0.75—1.00 for **5**) based on a series of ψ scans was carried out using the Enraf Nonius structure determination package.$^{19a)}$ The positions of the Ni, Pt, and S atoms for **3** and **5** were located by a direct method, and the remaining atoms were located in successive difference Fourier syntheses. All of the hydrogen atoms, except for the water molecules, were included in the refinement, but were restrained to ride on the atoms to which they were bonded (C–H or N–H = 0.95 Å, $U = 1.3U(C,N)$). The structure was refined by a full-matrix least-squares on F using anisotropic

Table 1. Crystal Data of $[Pt(bpy)\{Ni(aet)_2(bpy)\}](NO_3)_2\cdot H_2O$ (**3**) and $[Pt(phen)\{Ni(aet)_2(H_2O)_2\}]BrCl\cdot 1.5H_2O$ (**5**)

	3	**5**
Formula	$C_{24}H_{30}N_8S_2O_7NiPt$	$C_{16}H_{27}N_4S_2O_{3.5}BrClNiPt$
Fw	860.48	764.71
Cryst dimens/mm	$0.22 \times 0.10 \times 0.08$	$0.32 \times 0.10 \times 0.08$
Space group	$P\bar{1}$	$C2/c$
a/Å	12.640(3)	39.488(10)
b/Å	14.107(4)	5.363(1)
c/Å	9.382(2)	22.058(5)
α/deg	106.28(1)	
β/deg	99.08(2)	92.56(1)
γ/deg	65.93(2)	
V/Å^3	1464.5(7)	4666.6
Z	2	2
D_{calcd}/g cm^{-3}	1.95	2.18
μ/cm^{-1}	56.6	88.8
Transm factor	0.65—1.00	0.75—1.00
Scan type	ω–2θ	ω–2θ
θ range/deg	52.0	52.0
No. of reflcns measd	6123	5273
No. of reflcns used	5072	2335
No. of variables used	388	271
R (R_w)	0.028 (0.032)	0.074 (0.093)

thermal parameters for the non-hydrogen atoms. All of the calculations were performed on a VAX computer using the crystallographic package Molen.[19b)] The final atomic positional parameters for complexes **3** and **5** are given in Tables 2 and 3.[20)]

Results and Discussion

X-Ray Crystal Structures for 3 and 5. An X-ray structural analysis for **3** revealed the presence of a discrete divalent complex cation, two nitrate anions and a water molecule. Similarly, **5** consists of a discrete divalent complex cation, a chloride and a bromide anions, and one and a half water molecules. Perspective drawings of complex cations **3** and **5** are given in Figs. 1 and 2. Their selected bond distances and angles are listed in Tables 4 and 5.

Table 2. Final Atomic Coordinates and Equivalent Isotropic Thermal Parameters (B_{eq}/Å^2)[a)] for [Pt(bpy){Ni(aet)$_2$(bpy)}](NO$_3$)$_2$·H$_2$O (**3**)

Atom	x	y	z	B_{eq}
Pt	0.77147(2)	0.25222(2)	0.05078(3)	2.412(4)
Ni	0.73983(6)	0.51951(5)	0.12651(8)	2.36(1)
S(1)	0.8390(1)	0.3651(1)	0.2316(2)	2.94(3)
S(2)	0.6713(1)	0.3937(1)	−0.0569(2)	2.70(3)
N(1)	0.6079(4)	0.5603(4)	0.2707(6)	3.3(1)
N(2)	0.8763(4)	0.4660(4)	−0.0157(6)	3.1(1)
N(3)	0.8602(4)	0.1184(4)	0.1322(6)	3.0(1)
N(4)	0.7181(4)	0.1427(3)	−0.1022(6)	2.8(1)
N(5)	0.6465(4)	0.6558(4)	0.0456(6)	2.7(1)
N(6)	0.8037(4)	0.6301(4)	0.2665(5)	2.7(1)
C(1)	0.7441(6)	0.4129(5)	0.3861(7)	3.8(2)
C(2)	0.6181(6)	0.4737(5)	0.3400(9)	4.2(2)
C(3)	0.7667(6)	0.3729(5)	−0.2012(7)	3.6(2)
C(4)	0.8862(6)	0.3687(5)	−0.1346(8)	3.7(2)
C(5)	0.9369(6)	0.1124(5)	0.2503(8)	3.9(2)
C(6)	0.9999(7)	0.0167(5)	0.2934(8)	4.2(2)
C(7)	0.9823(7)	−0.0734(5)	0.2125(9)	4.3(2)
C(8)	0.9032(6)	−0.0689(5)	0.0893(8)	3.9(2)
C(9)	0.8428(5)	0.0294(5)	0.0525(7)	3.2(1)
C(10)	0.7602(5)	0.0437(4)	−0.0768(7)	3.0(1)
C(11)	0.7269(7)	−0.0374(5)	−0.1629(9)	4.4(2)
C(12)	0.6465(7)	−0.0156(6)	−0.2836(9)	4.9(2)
C(13)	0.6024(6)	0.0851(5)	−0.3123(8)	4.1(2)
C(14)	0.6415(6)	0.1628(5)	−0.2192(7)	3.4(1)
C(15)	0.5686(5)	0.6620(5)	−0.0692(7)	3.3(1)
C(16)	0.5112(6)	0.7537(5)	−0.1214(7)	3.6(2)
C(17)	0.5368(6)	0.8423(5)	−0.0514(8)	4.0(2)
C(18)	0.6161(6)	0.8388(5)	0.0712(8)	3.7(2)
C(19)	0.6698(5)	0.7428(4)	0.1159(7)	2.5(1)
C(20)	0.7568(5)	0.7292(4)	0.2412(7)	2.8(1)
C(21)	0.7888(6)	0.8113(5)	0.3288(9)	4.2(2)
C(22)	0.8693(7)	0.7915(6)	0.446(1)	4.9(2)
C(23)	0.9199(6)	0.6881(6)	0.4704(9)	4.4(2)
C(24)	0.8843(5)	0.6095(5)	0.3767(8)	3.5(2)
N(11)	0.2970(6)	0.8682(7)	0.5731(8)	6.8(2)
N(22)	0.1658(5)	0.3444(4)	0.2138(7)	4.0(1)
O(11)	0.3561(6)	0.7691(5)	0.5404(8)	7.3(2)
O(12)	0.3421(8)	0.9222(6)	0.6707(9)	9.7(3)
O(13)	0.2072(7)	0.9073(9)	0.5085(9)	14.5(4)
O(21)	0.1149(5)	0.3252(5)	0.0916(7)	6.2(2)
O(22)	0.2326(6)	0.2704(4)	0.2665(7)	6.5(2)
O(23)	0.1495(7)	0.4359(4)	0.2804(8)	8.2(2)
O(1w)	0.4096(5)	0.2521(5)	0.4819(6)	5.6(2)

a) B_{eq} denotes the equivalent isotropic temperature factors, $B_{eq} = (8\pi^2/3)\sum_i\sum_j U_{ij}a_i^* a_j^* \boldsymbol{a}_i \cdot \boldsymbol{a}_j$.

Table 3. Final Atomic Coordinates and Equivalent Isotropic Thermal Parameters (B_{eq}/Å^2)[a)] for [Pt(phen){Ni(aet)$_2$(H$_2$O)$_2$}]BrCl·1.5H$_2$O (**5**)

Atom	x	y	z	B_{eq}
Pt	0.62066(3)	−0.0793(2)	0.43065(5)	2.22(2)
Ni	0.5536(1)	−0.1193(7)	0.3235(2)	3.72(8)
S(1)	0.6060(2)	0.116(1)	0.3413(3)	3.0(1)
S(2)	0.5750(2)	−0.338(1)	0.4137(3)	2.6(1)
O(1)	0.5353(6)	0.122(4)	0.253(1)	6.3(6)
O(2)	0.5130(6)	−0.379(4)	0.307(1)	7.7(6)
N(1)	0.5821(9)	−0.321(5)	0.264(1)	6.0(8)
N(2)	0.5259(6)	0.083(6)	0.382(2)	7.6(9)
N(3)	0.6328(6)	−0.217(5)	0.5145(9)	3.4(5)
N(4)	0.6623(6)	0.141(5)	0.452(1)	3.3(5)
C(1)	0.6267(7)	−0.028(5)	0.281(1)	3.2(6)
C(2)	0.6193(9)	−0.295(7)	0.273(1)	4.1(7)
C(3)	0.5445(9)	−0.205(6)	0.461(1)	3.8(7)
C(4)	0.538(1)	0.062(8)	0.450(2)	7(1)
C(5)	0.6610(7)	−0.095(6)	0.544(1)	2.9(5)
C(6)	0.6739(7)	0.101(7)	0.510(1)	3.5(6)
C(7)	0.6749(8)	0.328(6)	0.420(1)	3.4(6)
C(8)	0.7011(8)	0.483(6)	0.442(2)	4.0(7)
C(9)	0.7141(7)	0.436(7)	0.500(2)	4.4(7)
C(10)	0.7011(8)	0.236(7)	0.535(1)	3.9(7)
C(11)	0.7135(7)	0.189(7)	0.595(2)	4.7(8)
C(12)	0.6998(8)	0.004(7)	0.627(1)	4.6(8)
C(13)	0.6724(7)	−0.142(8)	0.603(1)	4.1(8)
C(14)	0.6584(9)	−0.347(8)	0.632(1)	5.1(9)
C(15)	0.6310(9)	−0.478(6)	0.604(1)	4.1(7)
C(16)	0.6214(7)	−0.411(7)	0.544(1)	3.4(6)
Br	0.4341(1)	−0.013(1)	0.3763(2)	12.6(2)
Cl	0.7234(2)	−0.068(2)	0.3246(4)	4.7(2)
O(1w)	0.7098(5)	0.446(5)	0.226(1)	5.3(5)
O(2w)[b)]	0.467(1)	0.507(8)	0.388(2)	4(1)

a) B_{eq} denotes the equivalent isotropic temperature factors, $B_{eq} = (8\pi^2/3)\sum_i\sum_j U_{ij}a_i^* a_j^* \boldsymbol{a}_i \cdot \boldsymbol{a}_j$. b) Occupacy factor = 0.5.

Both complex cations **3** and **5** contain one Ni atom and one Pt atom to form the dinuclear complex. This is consistent with the plasma emission spectral analysis, which gave a value of Ni : Pt = 1 : 1. The Ni atom in **3** is surrounded by the two aet ligands and one bpy ligand to have an approximately octahedral geometry (Fig. 1). Its equatorial coordination

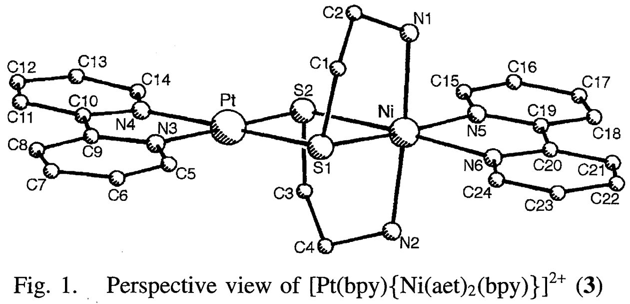

Fig. 1. Perspective view of [Pt(bpy){Ni(aet)$_2$(bpy)}]$^{2+}$ (**3**) with the atomic labeling scheme.

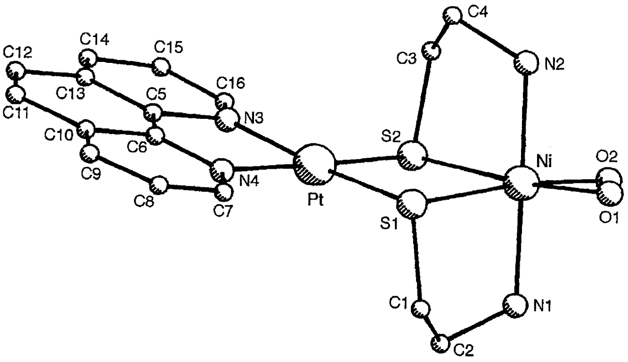

Fig. 2. Perspective view of $[Pt(phen)\{Ni(aet)_2(H_2O)_2\}]^{2+}$ (**5**) with the atomic labeling scheme.

Table 4. Selected Bond Distances (Å) and Angles (deg) for $[Pt(bpy)\{Ni(aet)_2(bpy)\}]^{2+}$ (**3**)

Pt–S(1)	2.297(2)	Ni–S(2)	2.435(2)
Pt–S(2)	2.297(2)	Ni–N(1)	2.106(6)
Pt–N(3)	2.053(5)	Ni–N(2)	2.103(6)
Pt–N(4)	2.050(5)	Ni–N(5)	2.086(5)
Ni–S(1)	2.424(2)	Ni–N(6)	2.086(5)
S(1)–Pt–S(2)	87.46(5)	S(2)–Ni–N(2)	85.3(2)
S(1)–Pt–N(3)	96.4(1)	S(2)–Ni–N(5)	98.9(1)
S(1)–Pt–N(4)	175.7(1)	S(2)–Ni–N(6)	174.5(2)
S(2)–Pt–N(3)	175.8(1)	N(1)–Ni–N(2)	175.4(2)
S(2)–Pt–N(4)	96.8(1)	N(1)–Ni–N(5)	91.2(2)
N(3)–Pt–N(4)	79.3(2)	N(1)–Ni–N(6)	92.3(2)
S(1)–Ni–S(2)	81.61(5)	N(2)–Ni–N(5)	93.1(2)
S(1)–Ni–N(1)	85.2(2)	N(2)–Ni–N(6)	90.2(2)
S(1)–Ni–N(2)	90.4(2)	N(5)–Ni–N(6)	78.1(2)
S(1)–Ni–N(5)	176.4(2)	Pt–S(1)–Ni	95.60(6)
S(1)–Ni–N(6)	101.7(1)	Pt–S(2)–Ni	95.32(5)
S(2)–Ni–N(1)	92.4(2)		

Table 5. Selected Bond Distances (Å) and Angles (deg) of $[Pt(phen)\{Ni(aet)_2(H_2O)_2\}]^{2+}$ (**5**)

Pt–S(1)	2.282(7)	Ni–S(2)	2.429(8)
Pt–S(2)	2.292(7)	Ni–O(1)	2.12(2)
Pt–N(3)	2.03(2)	Ni–O(2)	2.14(2)
Pt–N(4)	2.06(2)	Ni–N(1)	2.07(3)
Ni–S(1)	2.440(8)	Ni–N(2)	2.05(3)
S(1)–Pt–S(2)	88.3(3)	S(2)–Ni–O(2)	93.2(7)
S(1)–Pt–N(3)	173.7(7)	S(2)–Ni–N(1)	95.0(8)
S(1)–Pt–N(4)	95.8(7)	S(2)–Ni–N(2)	85.(1)
S(2)–Pt–N(3)	94.6(7)	O(1)–Ni–O(2)	92.6(9)
S(2)–Pt–N(4)	175.9(7)	O(1)–Ni–N(1)	92.(1)
N(3)–Pt–N(4)	81.0(1)	O(1)–Ni–N(2)	88.(1)
S(1)–Ni–S(2)	81.7(3)	O(2)–Ni–N(1)	89.(1)
S(1)–Ni–O(1)	93.5(7)	O(2)–Ni–N(2)	92.(1)
S(1)–Ni–O(2)	170.4(7)	N(1)–Ni–N(2)	179.(1)
S(1)–Ni–N(1)	83.7(9)	Pt–S(1)–Ni	94.7(3)
S(1)–Ni–N(2)	95.5(8)	Pt–S(2)–Ni	94.8(3)
S(2)–Ni–O(1)	171.2(7)		

sites are occupied by the two S atoms in aet and the two N atoms in bpy, and the axial sites are filled by the two N atoms in aet, forming *cis*(*S*)-$[Ni(aet)_2(bpy)]$ unit of the C_2 symmetry. Similarly, the Ni atom in **5** consists of the C_2-*cis*(*S*)-$[Ni(aet)_2(H_2O)_2]$ unit, that is, the bpy ligand in **3** is substituted by the two water molecules in **5** (Fig. 2). In both complex cations **3** and **5**, the Pt atoms have a square-planar geometry, as in the case of the starting complexes $[PtCl_2(L)]$ (L=bpy for **3**; phen for **5**), which have been coordinated by the two S atoms from the C_2-*cis*(*S*)-$[Ni(aet)_2\{bpy$ or $(H_2O)_2\}]$ unit and the two N atoms in bpy or phen. The PtS_2N_2 plane and the NiS_2N_2 equatorial plane in **3** are essentially coplanar, and its Pt–Ni distance is 3.4987(8) Å (Fig. 1). Therefore, this suggests that there is no interaction between the axial groups of the C_2-*cis*(*S*)-$[Ni(aet)_2(bpy)]$ unit and the vacant axial site of the Pt atom. The NiS_2O_2 equatorial plane in **5** is somewhat (7.0°) bent for the PtS_2N_2 plane (Fig. 2), but its Pt–Ni distance is 3.476(4) Å, which is a similar to that of **3**. It is noted that each complex cation **5** exists in the alternative arrangement to avoid an interaction with the neighboring cation (Fig. 3). These facts suggest that some repulsions in **5** occurs between the phen ligands to bend the Pt(II) plane against the Ni(II) plane. Accordingly, there also seem to be no interaction between the axial groups of the Ni(II) unit and the vacant axial site of the Pt atom.

Although the Ni–S bond distances (av. 2.430(2) Å) in **3** correspond well to those (av. 2.435(8) Å) in **5** (Tables 4 and 5), they are significantly longer than those on the *cis*(*S*)-$[Ni(aet)_2]$ units in $[Ni\{Ni(aet)_2\}_2]^{2+}$ (av. 2.155(5) Å).[3] This is in accordance with the fact that the six-coordinated Ni(II) complexes have a relatively weaker ligand field strength than the four-coordinated Ni(II) complexes.[21—24] The S–Ni–S angle (81.61(5)°) in **3** also corresponds well to that (81.7(3)°) observed in **5** (Tables 4 and 5). In contrast to the bond distances, these are very similar to that (81.4(2)°) observed in the square-planar *cis*(*S*)-$[Ni(aet)_2]$ unit of $[Ni\{Ni(aet)_2\}_2]^{2+}$.[3] It is noted, however, that the Pt–S–Ni bridging angles (av. 95.46(6)° for **3**; 95.75(3)° for **5**) approach the ideal tetrahedral angle of 109.5° compared with the corresponding Ni–S–Ni angles (av. 77.5(2)°) in $[Ni\{Ni(aet)_2\}_2]^{2+}$.[3] These

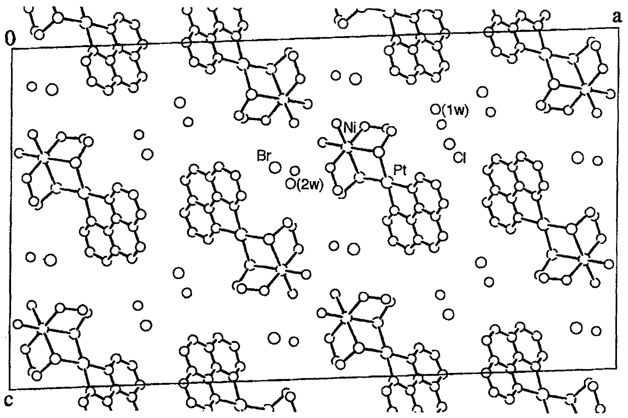

Fig. 3. Projection of crystal packing for $[Pt(phen)\{Ni(aet)_2(H_2O)_2\}]BrCl\cdot 1.5H_2O$ (**5**) viewed along *b* axis.

results seem to indicate that the S-bridged structures in **3** and **5** with the octahedral C_2-*cis*(*S*)-$[Ni(aet)_2\{bpy\ or\ (H_2O)_2\}]$ unit are less strained than that in $[Ni\{Ni(aet)_2\}_2]^{2+}$ with the square-planar *cis*(*S*)-$[Ni(aet)_2]$ units.

There are two possible optical isomers, Δ and Λ, for **3** and **5**, considering the absolute configurations of the *cis*(*S*)-$[Ni(aet)_2\{bpy\ or\ (H_2O)_2\}]$ unit. In crystals, **3** and **5** exist as the racemate, as shown in the crystal system (Table 1). Both of two bridging sulfur atoms in **3** and **5** are fixed to the R configuration for the Δ isomer and the S configuration for Λ isomer (Figs. 1 and 2). Further, two aet chelate rings take a *gauche* form with the λ conformation for the Δ isomer and the δ conformation for the Λ isomer.

Characterization. The elemental and plasma emission analytical data indicate that **1**, **2**, **5**, **6**, **9**, and **10** are consistent with the compositions of the expected planar–planar dinuclear structures for the Pt(II) and Ni(II) ions, $[Pt(L)\{Ni(aet)_2\}]X_2 \cdot nH_2O$ (X_2=Br_2, BrCl, $(NO_3)_2$), in which $[Ni(aet)_2]$ could function as S-donating metalloligands.[1—3,15] However, the magnetic moments of these complexes are not diamagnetic, but paramagnetic, as listed in Table 6. Namely, their values coincide well with those of **3** and **5**, whose structures were determined by X-ray analyses, due to the high-spin d^8 electron configuration of the Ni(II) ion, indicating the octahedral (or tetrahedral) geometry.[23,24] These therefore indicate that the possibility of planar–planar structures is excluded. The electronic absorption spectra of the pairs of **1** and **2**, **5** and **6**, or **9** and **10** are identical with each other over the whole region in aqueous solution. This means that these pairs of complexes take the same structures in solution as each other. All of the complexes exhibit weak absorption bands at about 10.5 and 17×10^3 cm^{-1} (Fig. 4 and Table 7). Similar absorption bands were also observed for such octahedral Ni(II) complexes as $[Ni(bpy)(H_2O)_4]^{2+}$,[25] $[Ni(bpy)_2(H_2O)_2]^{2+}$,[25] and $[Ni(bpy)_3]^{2+}$,[26] in which the bands have been assigned as spin-allowed d–d transitions, $^3A_{2g}\rightarrow{}^3T_{2g}$ and $^3A_{2g}\rightarrow{}^1T_{2g}$, respectively, from the lower energy side.[23—27] Further, the pairs of **1** and **2**, **5** and **6**, or **9** and **10** show the characteristic intense bands in the region of 29—45×10^3 cm^{-1}, which are assigned as the π system in the ligands (Fig. 4 and Table 7);[25,26] also the absorption intensities of **1** and **2** are about half for those of $[Pt(bpy)\{Ni(aet)_2(bpy)\}]^{2+}$ (**3**; Fig. 4 and Table 7). A similar trend was also observed for **5**, **6**, and **7** or **9**, **10**, and **11**, respectively (Table 7). Accordingly, these facts reasonably indicate that **1**, **2**, **5**, **6**, **9**, and **10** take dinuclear structures in solution, $[Pt(L)\{Ni(aet)_2(H_2O)_2\}]^{2+}$ (L = bpy for **1** and **2**; phen for **5** and **6**; dmbpy for **9** and **10**). These results are also supported by the molar conductivity in the solution that **1** in water exhibited value of 228 S cm^2 mol^{-1}, which are in good agreement with that (216 S cm^2 mol^{-1}) of the 1 : 2 electrolyte of $[Pt(bpy)\{Ni(aet)_2(bpy)\}](NO_3)_2$ (**3**).

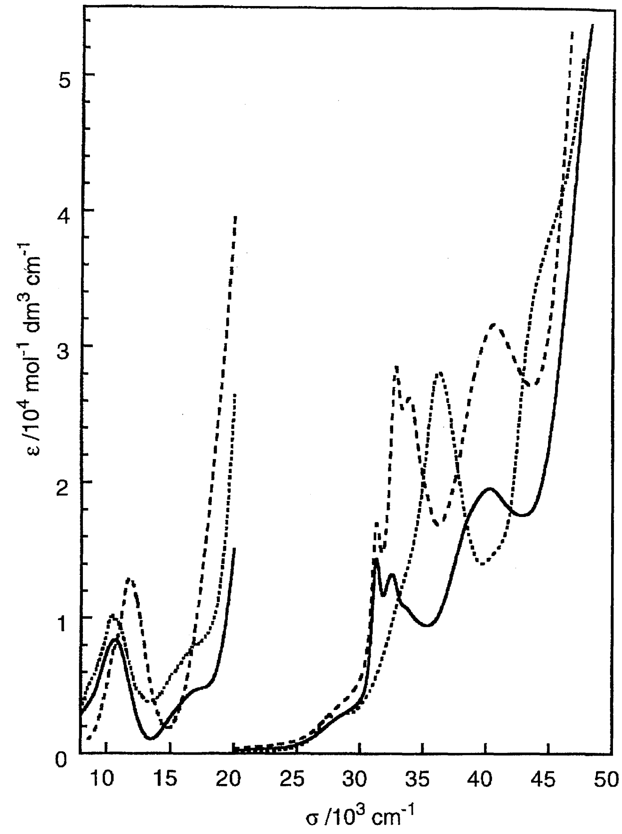

Fig. 4. Electronic absorption spectra of $[Pt(L)\{Ni(aet)_2(H_2O)_2\}]^{2+}$ L=bpy (**1**; —) and phen (**5**; ····), and $[Pt(bpy)\{Ni(aet)_2(bpy)\}]^{2+}$ (**3**; - - -).

$[Pt(bpy)\{Ni(aet)_2(bpy)\}]^{2+}$ (**3**) is easily obtained by the

Table 6. Magnetic Moments (μ_{eff})[a] and Electrochemical Data (*E*/V)[b]

Complex	μ_{eff}	E_{pc}	E_{pa}	$E^{\circ\prime}$ [c]
$[Pt(bpy)\{Ni(aet)_2(H_2O)_2\}]^{2+}$ (**1**)	3.23	0.610	0.675	0.643
$[Pt(bpy)\{Ni(aet)_2(NO_3)(H_2O)\}]^{+}$ (**2**)	3.13			
$[Pt(bpy)\{Ni(aet)_2(bpy)\}]^{2+}$ (**3**)	3.08	0.525	0.590	0.558
$[Pt(phen)\{Ni(aet)_2(H_2O)_2\}]^{2+}$ (**5**)	3.04	0.625	0.685	0.655
$[Pt(phen)\{Ni(aet)_2(NO_3)(H_2O)\}]^{+}$ (**6**)	3.16			
$[Pt(phen)\{Ni(aet)_2(phen)\}]^{2+}$ (**7**)	3.17	0.535	0.598	0.567
$[Pt(dmbpy)\{Ni(aet)_2(H_2O)_2\}]^{2+}$ (**9**)	3.05	0.610	0.674	0.642
$[Pt(dmbpy)\{Ni(aet)_2(NO_3)(H_2O)\}]^{+}$ (**10**)	3.45			
$[Pt(dmbpy)\{Ni(aet)_2(dmbpy)\}]^{2+}$ (**11**)	3.17	0.494	0.560	0.527
$[Pd(phen)\{Ni(aet)_2(phen)\}]^{2+}$ (**12**)	3.23			

a) 296 K; B. M. b) 296 K; 0.1 mol dm^{-3} Na_2SO_4 aqueous solution; scan rate 100 mV s^{-1}; V vs. Ag/AgCl (3 M NaCl) (1 M = 1 mol dm^{-3}). c) $E^{\circ\prime}=(E_{pc}+E_{pa})/2$.

Table 7. Absorption Spectral Data ($\sigma/10^3$ cm^{-1} ($\varepsilon/10^3$ mol^{-1} dm^3 cm^{-1}))

$[Pt(bpy)\{Ni(aet)_2(H_2O)_2\}]^{2+}$ (**1**)	10.64 (16.7)	17.3 (9.4, sh)	28.7 (3050, sh)	31.30 (14350)	32.53 (13220)
	33.7 (10800, sh)	40.24 (19520)			
$[Pt(bpy)\{Ni(aet)_2(bpy)\}]^{2+}$ (**3**)	10.7 (16.0, sh)	11.79 (25.9)	28.3 (3520, sh)	31.29 (16960)	32.84 (28490)
	33.86 (26230)	40.60 (31650)			
$[Pt(bpy)\{Ni(aet)_2(phen)\}]^{2+}$ (**4**)	10.5 (14.1, sh)	11.74 (24.6)	29.09 (4240)	31.30 (16660)	32.63 (17560)
	34.28 (21150)	37.20 (44090)	44.4 (53400, sh)		
$[Pt(phen)\{Ni(aet)_2(H_2O)_2\}]^{2+}$ (**5**)	10.42 (20.6)	16.8 (16.1, sh)	27.55 (2800)	29.04 (2980)	36.23 (28120)
	44.5 (37000, sh)				
$[Pt(phen)\{Ni(aet)_2(phen)\}]^{2+}$ (**7**)	10.6 (18.8, sh)	12.05 (27.9)	27.55 (3470)	29.02 (4470)	37.04 (51860)
	44.44 (65330)				
$[Pt(phen)\{Ni(aet)_2(bpy)\}]^{2+}$ (**8**)	10.6 (18.4, sh)	11.79 (29.2)	27.52 (3360)	32.92 (25860)	34.22 (29160)
	36.04 (34630)	40.6 (2500, sh)	44.1 (39600, sh)		
$[Pt(dmbpy)\{Ni(aet)_2(H_2O)_2\}]^{2+}$ (**9**)	10.64 (18.2)	17.09 (11.1)	29.2 (3290, sh)	31.55 (14740)	32.87 (14360)
	34.04 (12320, sh)	40.10 (22870)			
$[Pt(dmbpy)\{Ni(aet)_2(dmbpy)\}]^{2+}$ (**11**)	10.5 (20.7, sh)	11.59 (27.2)	29.1 (4340, sh)	31.53 (17870)	33.00 (26470)
	34.11 (24040)	40.21 (33320)			
$[Pd(phen)\{Ni(aet)_2(phen)\}]^{2+}$ (**12**)	10.5 (27.0, sh)	11.84 (37.8)	20.01 (186)	29.07 (4650)	34.3 (25350, sh)
	37.05 (65330)	44.64 (95220)			

reaction of $[Pt(bpy)\{Ni(aet)_2(H_2O)_2\}]^{2+}$ (**1**) with bpy. Similar reactions of **5** with phen and **9** with dmbpy also gave **7** and **11**, respectively. The absorption spectral behavior of **11** is quite similar to that of $[Pt(bpy)\{Ni(aet)_2(bpy)\}]^{2+}$ over the whole region, as in the case of **1** and **9** (Table 7). These facts suggest that **11** is assignable to $[Pt(dmbpy)\{Ni(aet)_2(dmbpy)\}]^{2+}$. This is supported by the fact that in the d–d transition band region of 10—13×10^3 cm^{-1}, the absorption bands (11.79 and 11.59×10^3 cm^{-1}) of **3** and **11** appear to more higher energies than those (10.64×10^3 cm^{-1}) of $[Pt(L)\{Ni(aet)_2(H_2O)_2\}]^{2+}$ (L = bpy for **1**; dmbpy for **9**). This corresponds to the ligand field strength around the Ni(II) units;[23,24] that is, **1** and **9** are the $(S)_2(N)_2(O)_2$ chromophore with the *cis·cis·cis* geometry, but **3** and **11** are the $(S)_2(N)_4$ chromophore with the *cis*(*S*) geometry. Similar relationship was also observed for **5** and **7**. These facts indicate, accordingly, that **7** can be assigned to $[Pt(phen)\{Ni(aet)_2(phen)\}]^{2+}$.

In the IR spectra, $[Pt(bpy)\{Ni(aet)_2(bpy)\}](NO_3)_2$ (**3**) gives strong stretching bands at 1371 and 1345 cm^{-1}, which do not appear for the corresponding bromide salt ($(Br)_2$ salt of **3**). Similar strong stretching bands were also observed for $[Pt(L)\{Ni(aet)_2(L)\}](NO_3)_2$ (L = phen (**7**), 1374 cm^{-1}; dmbpy (**11**), 1362 cm^{-1}), but not for **5**, **7**, and **9**. This suggests the existence of free NO_3^- ions. In addition to the strong stretching bands for the free NO_3^- ions, another strong band appears at 1328 cm^{-1} for **2** and at 1320 cm^{-1} for **10**, indicating the coordinated monodentate NO_3^-. Similar bands were not observed for the $(NO_3)_2$ and $(Br)_2$ salts of **3** and **7**, **5**, **9** and **11**. A similar trend was also observed for the ionic nitrate and the monodentate nitrate for Ni(II) complexes.[28,29] These facts and the elemental analytical data seem to indicate that in the solid state one of the nitrates in **2**, **6**, and **10** readily coordinates to the Ni(II) ion to form dinuclear structures of $[Pt(L)\{Ni(aet)_2(NO_3)(H_2O)\}](NO_3)\cdot nH_2O$ (L=bpy for **2**; phen for **6**; dmbpy for **10**). Three geometries, C_1-*cis*(*O*), C_2-*cis*(*O*) and *trans*(*O*), are possible for the *cis*(*S*)-$[Ni(aet)_2(H_2O)_2]$ or *cis*(*S*)-$[Ni(aet)_2(NO_3)(H_2O)]$ units. Molecular model examinations reveal that a significant strain on the coordinated sulfur atoms exists in the C_1-*cis*(*O*) and *trans*(*O*) geometries, when the Ni(II) equatorial plane is coplanar with the Pt(II) one to avoid an axial–axial interaction. Taking into account these examinations, the crystal structures of **3** and **5**, and the substitution reactions of $[Pt(L)\{Ni(aet)_2(H_2O)_2\}]^{2+}$ with L′ (L, L′ = bpy, phen, dmbpy), suggest that the C_2-*cis*(*O*) geometry around the Ni(II) units is retained not only in the solid state, but also in solution, although the coordinated nitrate anion is substituted by the water molecule in aqueous solution.

The reaction of $[Pt(bpy)\{Ni(aet)_2(H_2O)_2\}]^{2+}$ (**1**) with phen and **5** with bpy also gave **4** and **8**, respectively. The absorption spectra of **4** and **8** are more complicated in the region of the π system in the ligands, although their d–d transition bands (11.74×10^3 cm^{-1} for **4**; 11.79×10^3 cm^{-1} for **8**) correspond well with those of $[Pt(L)\{Ni(aet)_2(L)\}]^{2+}$ (L = bpy (**3**), phen (**7**), dmbpy (**11**)) containing the $(S)_2(N)_4$ chromophore (Fig. 5 and Table 7). However, their absorption behavior could be represented by the consideration that the absorption bands of the π system due to the Pt(II)–L (L = bpy or phen) in **3** and **7** appear more at the lower energy side than those due to the corresponding Ni(II)–L without the π–π interaction between bpy and phen, depending on the results that the Pt(II)–L bond is stronger than the Ni(II)–L bond. Therefore, these facts and the reactivities suggest that **4** can be assigned to $[Pt(bpy)\{Ni(aet)_2(phen)\}]^{2+}$ and **8** to $[Pt(phen)\{Ni(aet)_2(bpy)\}]^{2+}$. Namely, it is exhibited that the additional L easily substitutes for two water molecules, which coordinate to the Ni(II) atom without an exchange of L, which is coordinated to the Pt(II) atom.

A plasma emission analysis of **12** gave a value of Pd : Ni = 1 : 1, and an elemental analysis proves that the formula of **12** is consistent with that of a dinuclear structure in $[Pt(phen)\{Ni(aet)_2(phen)\}]^{2+}$ (**7**). Further, the absorption spectral behavior of **12** is quite similar to that of **7** over the whole region. Accordingly, it is reasonable to assume that **12** is $[Pd(phen)\{Ni(aet)_2(phen)\}]^{2+}$.

The reaction of $[Ni(aet)_2]$ with $[PtCl_2(L)]$ (L = bpy, phen,

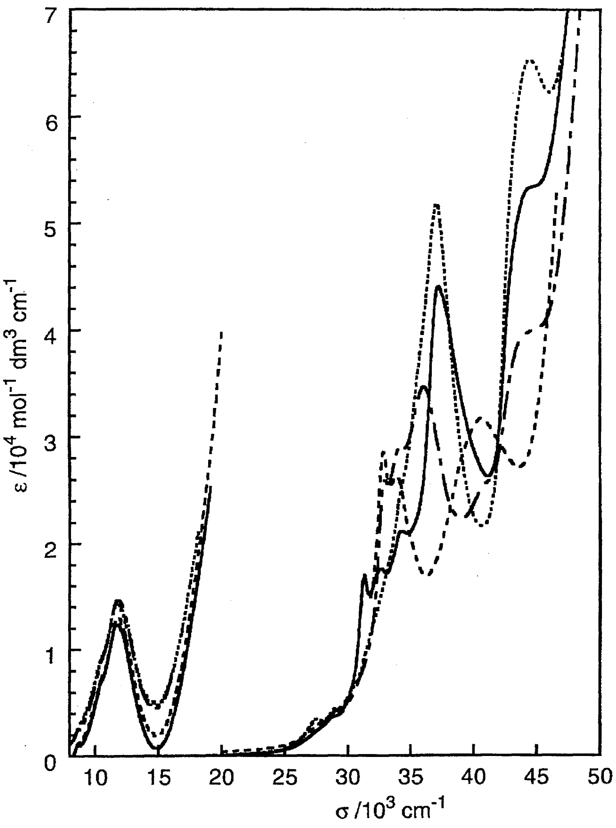

Fig. 5. Electronic absorption spectra of $[Pt(bpy)\{Ni(aet)_2(L)\}]^{2+}$ L=phen (**4**; —) and bpy (**3**; - - -), and $[Pt(phen)\{Ni(aet)_2(L)\}]^{2+}$ L=bpy (**8**; – • –) and phen (**7**; ••••).

dmbpy) in water readily gave S-bridged dinuclear complexes, $[Pt(L)\{Ni(aet)_2(H_2O)_2\}]^{2+}$ (**1**, **5**, and **9**), in which a square-planar $[Ni(aet)_2]$ converts to an octahedral $[Ni(aet)_2(H_2O)_2]$ unit. However, $[Ni(aet)_2]$ did not react with water nor 2,2′-bipyridine under several conditions (ca. 80 °C for several hours) without $[PtCl_2(L)]$, and the octahedral complex $[Ni(aet)_2\{(H_2O)_2$ or bpy$\}]$ could not be formed. This means that $[PtCl_2(L)]$ is necessary for conversion to the octahedral Ni(II) unit. The treatment of $[Pt(L)\{Ni(aet)_2(H_2O)_2\}]^{2+}$ with L′ or the addition of L′ to the reaction solution for $[Pt(L)\{Ni(aet)_2(H_2O)_2\}]^{2+}$ afforded quantitatively the corresponding complexes $[Pt(L)\{Ni(aet)_2(L')\}]^{2+}$ (**3**, **4**, **7**, **8**, and **11**). Similarly, the addition of phen to the reaction solution of $[Ni(aet)_2]$ with $[PdCl_2(phen)]$ affords quantitatively an S-bridged dinuclear complex $[Pd(phen)\{Ni(aet)_2(phen)\}]^{2+}$ (**12**). In the Pd(II) complexes, however, $[Pd(phen)\{Ni(aet)_2(H_2O)_2\}]^{2+}$, corresponding to the Pt(II) dinuclear complex was not isolated. Furthermore, when $[PdCl_2(bpy)]$ was employed instead of $[PdCl_2(phen)]$, the dinuclear complex was not formed, but the hexanuclear complex $[Pd_2\{Ni(aet)_2\}_4]^{4+}$[15] was obtained in good yield, even in a mild condition, suggesting that $[PdCl_2(L)]$ is relatively more reactive than $[PtCl_2(L)]$. Accordingly, conversion of the square-planar $[Ni(aet)_2]$ to the octahedral $[Ni(aet)_2(L)]$ seems to obviously be caused by the formation of an S-bridged structure with stable square-planar mononuclear complexes.

The present type of dinuclear complexes are optically active, as mentioned in discussions concerning the X-ray structures of **3** and **5**. Although the optical resolutions for all of the complexes have been attempted, they could not be achieved by some methods. In the column chromatographic technique, the existence of an interaction with the exchange resins results in a decomposition of the complexes, although racemic $[Pt(L)\{Ni(aet)_2(L')\}]^{2+}$ is stable in aqueous solution. In fractional crystallizations for the solubility of any solvents, further, the racemization accompanied by a M–S cleavage seems to easily occur for the present dinuclear complexes, since the Ni(II) complexes are relatively active for substitution, and isomerization accompanied by a M–S cleavage has been recognized even for a more stable trinuclear complex $[Co\{Ir(aet)_3\}_2]^{3+}$ with the two S-donating tridentate metalloligands.[30]

Electrochemistry. Electrochemical experiments were performed by cyclic voltammetry (CV). The representative cyclic voltammogram for the $Pt^{II}Ni^{II}$ dinuclear complexes are shown in Fig. 6, and all of their data are listed in Table 6. The cyclic voltammogram was indicated at 0 V with a positive scan, and yielded one oxidation wave (E_{pa}) coupled with one reduction wave (E_{pc}). No other redox couple was observed in the potential region of +1.0 to −1.0 V (vs. Ag/AgCl). The peak current is proportional to the square root of the scan rate, and the ratio of the cathodic peak current to the anodic one is nearly unity for each of the dinuclear Pt(II)–Ni(II) complexes. At a scan rate of 100 mV s^{-1}, the observed peak separation ($\Delta E_p = E_{pa} - E_{pc}$) is 60—72 mV for a series of $[Pt(L)\{Ni(aet)_2(H_2O)_2\}]^{2+}$ and $[Pt(L)\{Ni(aet)_2(L')\}]^{2+}$. These results indicate that the redox reactions are electrochemically quasi-reversible. In the redox process, the differences for the coordination spheres about the Ni(II) ion affect the formal potentials (Table 6). Taking the configurations about the Ni(II) ion into consideration, each of the formal potentials seem to correspond to the redox potential of the Ni(II)/Ni(III)

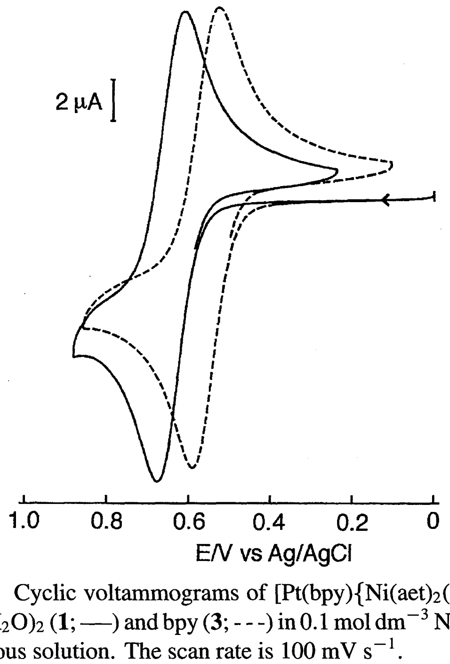

Fig. 6. Cyclic voltammograms of $[Pt(bpy)\{Ni(aet)_2(L)\}]^{2+}$ L=$(H_2O)_2$ (**1**; —) and bpy (**3**; - - -) in 0.1 mol dm^{-3} Na_2SO_4 aqueous solution. The scan rate is 100 mV s^{-1}.

couple for the [Ni(aet)$_2$(H$_2$O)$_2$] and [Ni(aet)$_2$(L)] units. The redox couples for [Pt(L){Ni(aet)$_2$(H$_2$O)$_2$}]$^{2+}$ are ca. 0.1 V more positive than those for [Pt(L){Ni(aet)$_2$(L$'$)}]$^{2+}$ (Fig. 6 and Table 6). This indicates that replacement of (H$_2$O)$_2$ by diimine ligand L stabilizes the Ni(III) oxidation state.

This work was supported by a Grant-in-Aid for Scientific Research No. 07454172 from the Ministry of Education, Science and Culture.

References

1) D. C. Jicha and D. H. Busch, *Inorg. Chem.*, **1**, 872 (1962).

2) D. C. Jicha and D. H. Busch, *Inorg. Chem.*, **1**, 878 (1962).

3) C. H. Wei and L. F. Dahl, *Inorg. Chem.*, **9**, 1878 (1970).

4) R. J. Arts, E. L. Blinn, and D. S. Newman, *J. Inorg. Nucl. Chem.*, **35**, 2831 (1973).

5) R. W. Hay, A. L. Galyer, and G. A. Lawrance, *J. Chem. Soc., Dalton Trans.*, **1976**, 939.

6) M. G. B. Drew, D. A. Rice, and K. M. Richards, *J. Chem. Soc., Dalton Trans.*, **1980**, 2075.

7) H. Barrera, J. Suades, M. C. Perucard, and J. L. Brianso, *Polyhedron*, **3**, 839 (1984).

8) M. A. Turner, W. E. Driessen, and J. Reedijk, *Inorg. Chem.*, **29**, 3331 (1990).

9) G. J. Colpas, M. Kumar, R. O. Day, and M. J. Maroney, *Inorg. Chem.*, **29**, 4779 (1990).

10) D. Kang, M. Poor, E. L. Blinn, and P. M. Trichel, *Inorg. Chim. Acta*, **168**, 209 (1990).

11) D. K. Mills, Y. M. Hsiao, P. J. Farmer, E. V. Atnip, J. H. Reibenspies, and M. Y. Darensbourg, *J. Am. Chem. Soc.*, **113**, 1421 (1991).

12) P. J. Farmer, T. Solouki, D. K. Mills, T. Soma, H. Russell, J. H. Reibenspies, and M. Y. Darensbourg, *J. Am. Chem. Soc.*, **114**, 4601 (1992).

13) T. Tuntulani, J. H. Reibenspies, P. J. Farmer, and M. Y. Darensbourg, *Inorg. Chem.*, **31**, 3497 (1992).

14) G. J. Colpas, P. O. Day, and M. J. Maroney, *Inorg. Chem.*, **31**, 5053 (1992).

15) T. Konno, K. Yonenobu, J. Hidaka, and K. Okamoto, *Inorg. Chem.*, **33**, 861 (1994).

16) T. Konno, Y. Yoshinari, and K. Okamoto, *Chem. Lett.*, **1995**, 989.

17) N. Baidya, D. Ndreu, M. Olmstead, and K. Mascharak, *Inorg. Chem.*, **30**, 2448 (1991).

18) R. H. Herber, M. Croft, M. J. Coyer, B. Bilash, and A. Sahiner, *Inorg. Chem.*, **33**, 2422 (1994).

19) a) "Enraf Nonius Structure Determination Package (SDP)," Enraf–Nonius, Delft, The Netherlands (1978); b) C. K. Fair, Molen, "Interactive Structure Solution Procedure," Enraf–Nonius, Delft, The Netherlands (1990).

20) Lists of structure factors, hydrogen atoms coordinates, bond distances and angles, and anisotropic thermal parameters for non-hydrogen atoms are deposited as Document No. 71030 at the Office of the Editor of Bull. Chem. Soc. Jpn.

21) N. Baidya, M. Olmstead, and K. Mascharak, *Inorg. Chem.*, **30**, 929 (1991).

22) T. Konno, K. Okamoto, and J. Hidaka, *Acta Crystallogr., Sect. C*, **C49**, 222 (1993); *Inorg. Chem.*, **30**, 2448 (1991).

23) F. A. Cotton and G. Wilkinson, "Advanced Inorganic Chemistry," John Wiley & Sons, New York (1987).

24) B. E. Douglas, D. H. McDaniel, and J. J. Alexander, "Concepts and Models of Inorganic Chemistry," 3rd ed, John Wiley & Sons, New York (1994).

25) S. Bunel, L. Gil, E. Moraga, and H. Bobadilla, *Inorg. Chim. Acta*, **4**, 415 (1970).

26) R. A. Palmer and T. S. Piper, *Inorg. Chem.*, **5**, 864 (1966).

27) H.-J. Krüger and R. H. Holm, *J. Am. Chem. Soc.*, **112**, 2955 (1990).

28) N. F. Curtis and Y. M. Curtis, *Inorg. Chem.*, **4**, 804 (1965).

29) K. Nakamoto, "Infrared and Raman Spectra of Inorganic and Coordination Compounds," 3rd ed, John Wiley & Sons, New York (1987).

30) T. Konno, K. Nakamura, K. Okamoto, and J. Hidaka, *Bull. Chem. Soc. Jpn.*, **66**, 2582 (1993).